Supporting Information

Charge-enriched RuO_2 nanoparticles decorating TiO_2 with Ti defects to promote oxygen evolution reaction in acidic media

Ye Wang,[a] Yixin Hao,[a] Luqi Wang,[a] Chunsheng Li,[bc] Jianwei Ren,[d] Yan Sun,[bc] Feng Hu*[a], Linlin Li[a], and Shengjie Peng*[a]

[a]College of Materials Science and Technology, Nanjing University of Aeronautics and Astronautics, Nanjing 210016, China. E-mail: pengshengjie@nuaa.edu.cn
[b]School of Chemistry and Life Sciences, Suzhou University of Science and Technology, Suzhou City, Jiangsu Province 215009 (P. R. China)
[c]Key Laboratory of Advanced Electrode Materials for Novel Solar Cells for Petroleum and Chemical Industry of China, Suzhou University of Science and Technology, Suzhou City, Jiangsu Province 215009 (P. R. China)
[d]Department of Mechanical Engineering Science, University of Johannesburg, Cnr Kingsway and University Roads, Auckland Park, 2092, Johannesburg, South Africa.

TOF calculation

Turnover frequency (TOF) was calculated via the following formula according to previous reports.

$$\text{TOF per site} = \frac{\#\ \text{Total Oxygen Turn Over/cm}^2\ \text{geometric area}}{\#\ \text{Surface Sites/cm}^2\text{geometric area}}$$

The total number of oxygens turnovers was calculated from the current density using the following equation:

$$\#O_2 = \left(j\frac{\text{mA}}{\text{cm}^2}\right)\left(\frac{1\text{C s}^{-1}}{1000\ \text{mA}}\right)\left(\frac{1\ \text{mol s}^{-1}}{1000\ \text{mA}}\right)\left(\frac{1\ \text{mol O}_2}{4\ \text{mol e}^-}\right)\left(\frac{6.022\times10^{23}\text{O}_2\ \text{molecules}}{1\ \text{mol O}_2}\right) = J\times1.56\times10^{15}\frac{\text{O}_2/\text{s}}{\text{cm}^2}\text{per}\frac{\text{mA}}{\text{cm}^2}$$

The Ru content of d-TiO_2/RuO_2 is determined by the ICP. The mass loading on the electrode is ~0.30 mg cm^{-2}. Thus, n is calculated as:

$$n(\text{d - TiO2/RuO2}) = \frac{2.42\%\times0.30\frac{\text{mg}}{\text{cm}^2}}{58.93\frac{\text{g}}{\text{mol}}} = 1.23\times10^{-7}\ \text{mol/cm}^2$$

$$N^{\text{d - TiO2/RuO2}}_{\text{active}} = 6.022\times10^{23}\text{mol}^{-1}\times1.23\times10^{-7}\text{mol/cm}^2 = 7.407\times10^{16}\ \text{atoms/cm}^2$$

$$\text{TOF} = \frac{|J|\times1.56\times10^{15}\frac{\text{O}_2/\text{s}}{\text{cm}^2}\text{per}\frac{\text{mA}}{\text{cm}^2}}{N^{\text{d - TiO2/RuO2}}_{\text{active}}}$$

Mass activity calculation

The mass activity ($j_{\text{mass activity}}$) of the d-TiO_2/RuO_2, TiO_2/RuO_2 and RuO_2 catalysts was determined using the following formula:

$$j_{mass\ activity} = \frac{j_{geo} \times A_{geo}}{m_{Ru}}$$

where m_{Ru} is the calculated Ru mass loaded onto carbon paper based on the results of ICP-OES analysis, A_{geo} is the geometric area and j_{geo} is the geometric current density.

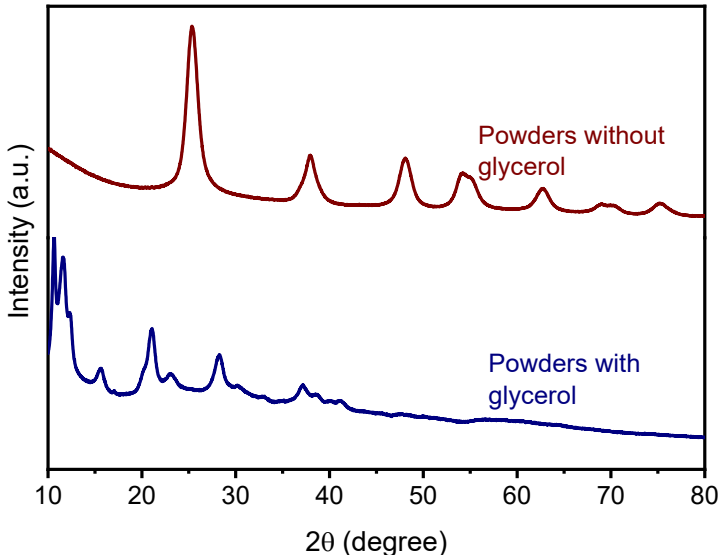

Fig. S1. XRD patterns of precursor powders synthesized with and without glycerol, respectively.

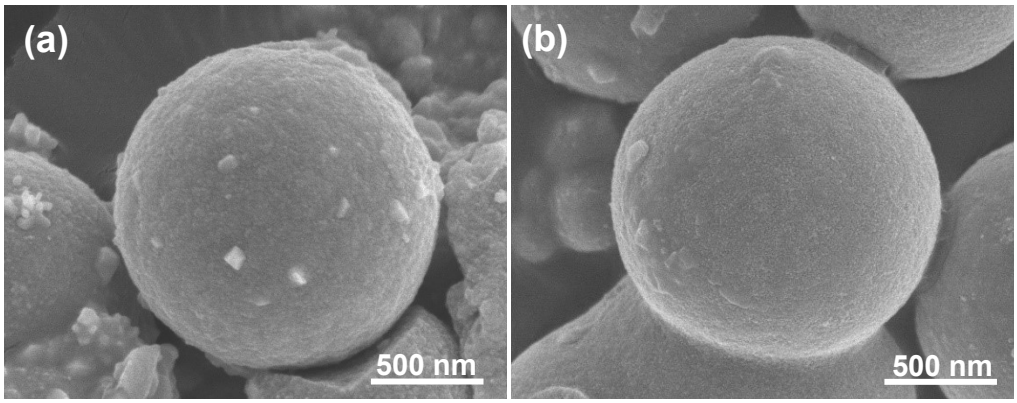

Fig. S2. SEM images of (a) TiO_2/RuO_2 and (b) TiO_2, respectively.

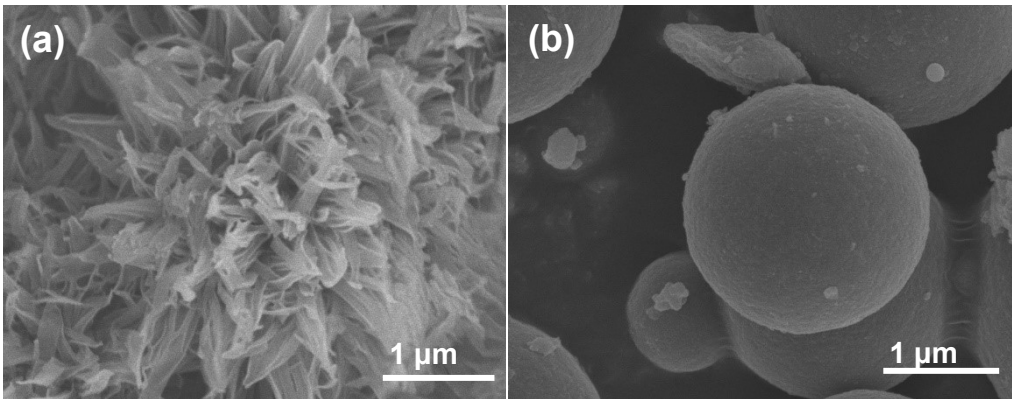

Fig. S3. SEM images of precursor powders synthesized (a) with and (b) without glycerol, respectively.

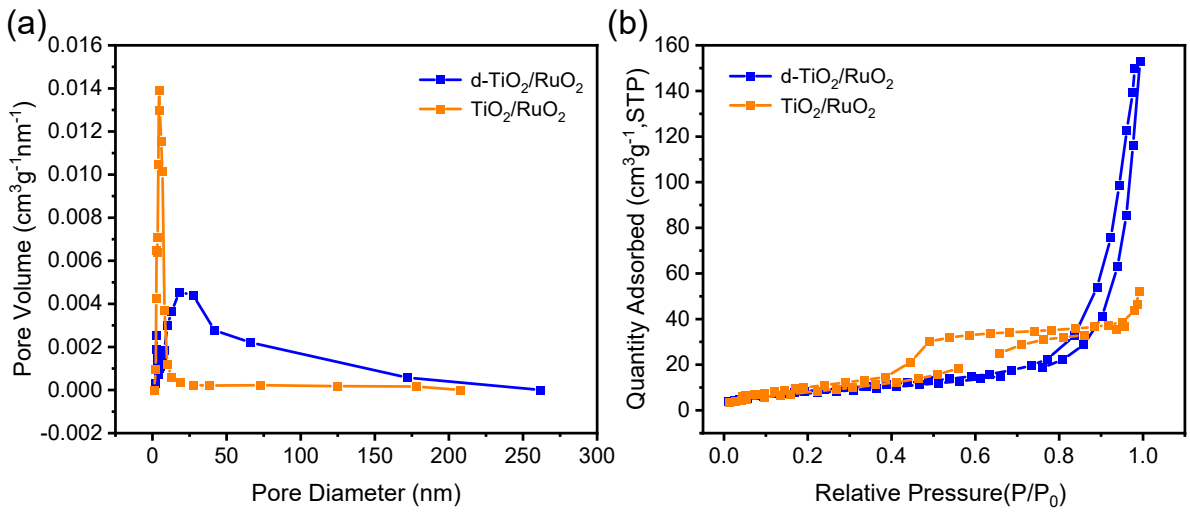

Fig. S4. (a) N_2 adsorption/desorption isotherm and (b) the corresponding pore size distribution of d-TiO_2/RuO_2 and TiO_2/RuO_2, respectively.

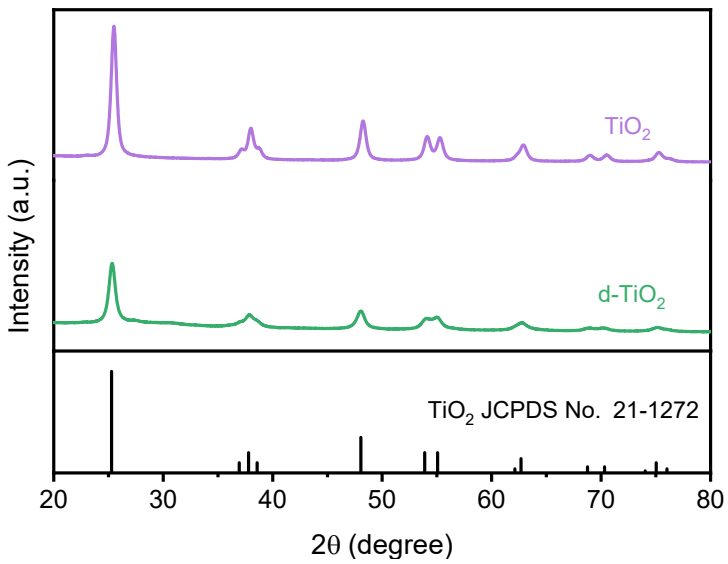

Fig. S5. XRD patterns of d-TiO_2 and TiO_2, respectively.

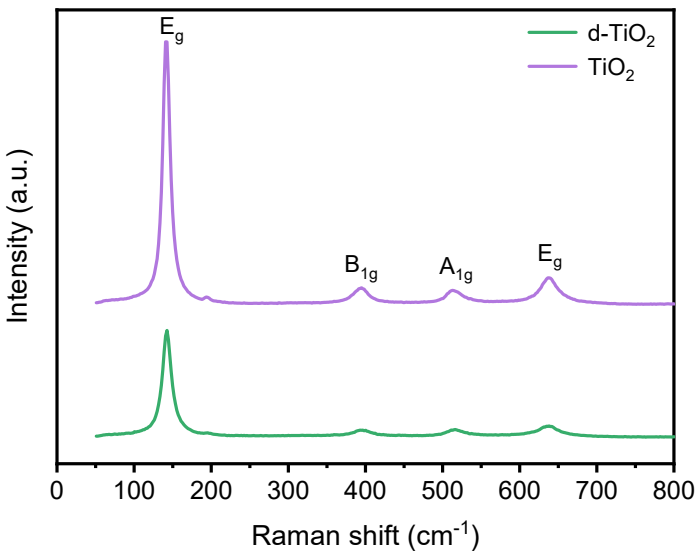

Fig. S6. Raman spectra of d-TiO_2 and TiO_2, respectively.

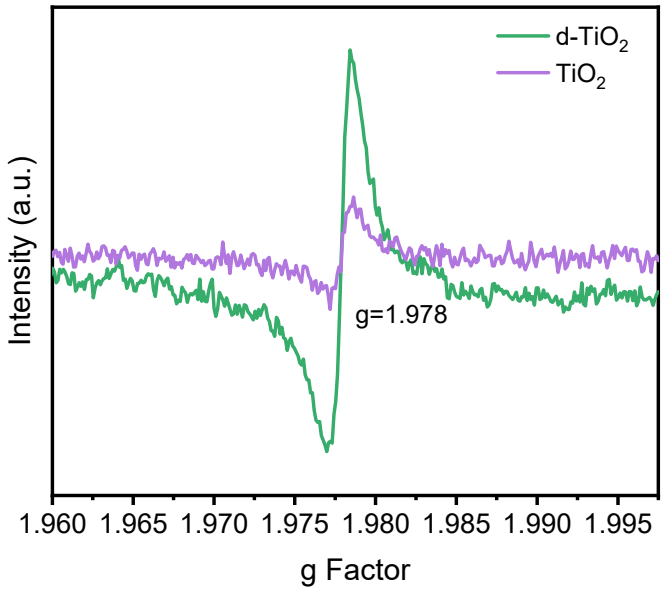

Fig. S7. EPR spectra of d-TiO_2 and TiO_2, respectively.

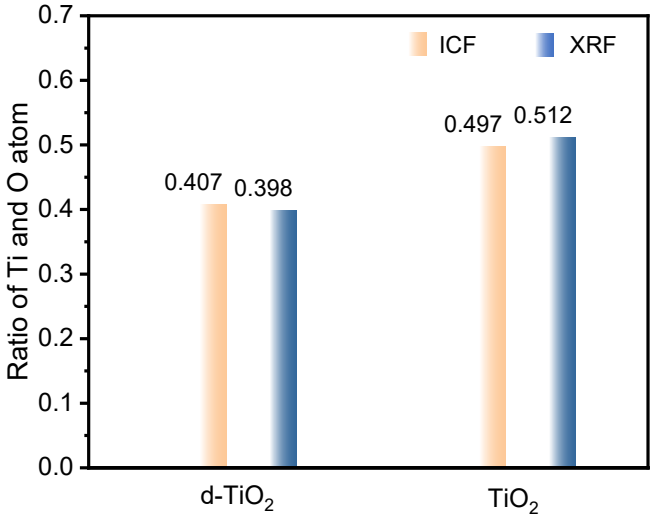

Fig. S8. The ratios of Ti and O atoms of TiO_2 and d-TiO_2 calculated by X-ray fluorescence spectrometer (XRF) and inductively coupled plasma (ICP) analysis, respectively.

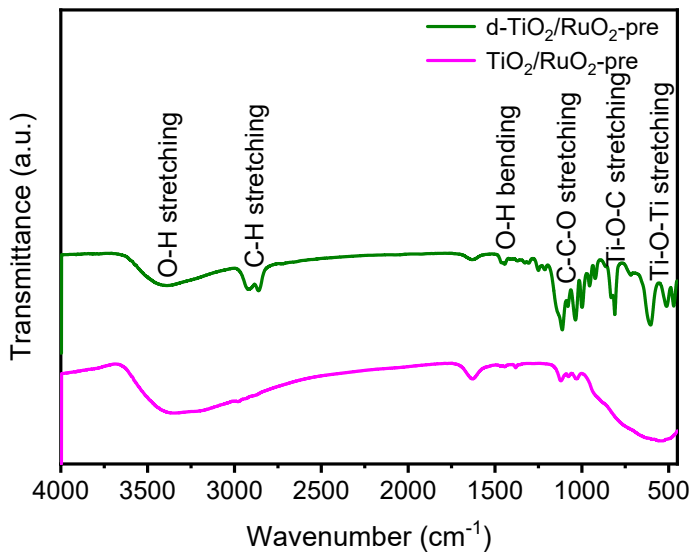

Fig. S9. FTIR spectra of d-TiO_2/RuO_2-pre and TiO_2/RuO_2-pre, respectively.

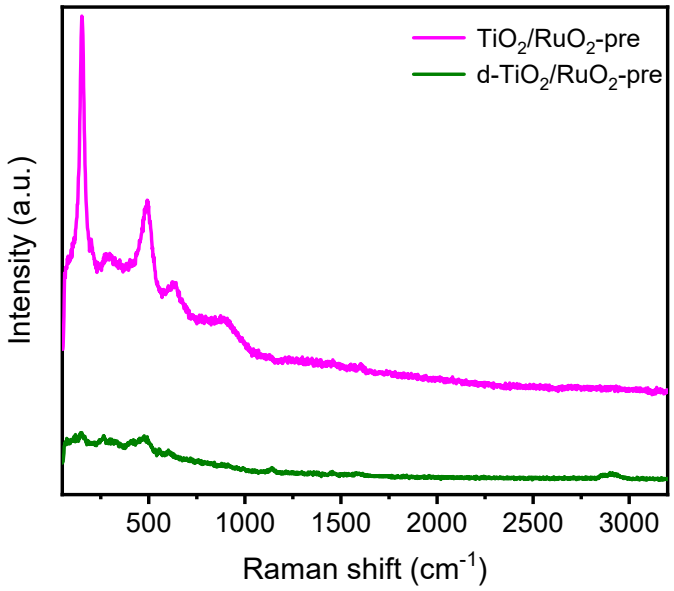

Fig. S10. Raman spectra of d-TiO_2/RuO_2-pre and TiO_2/RuO_2-pre, respectively.

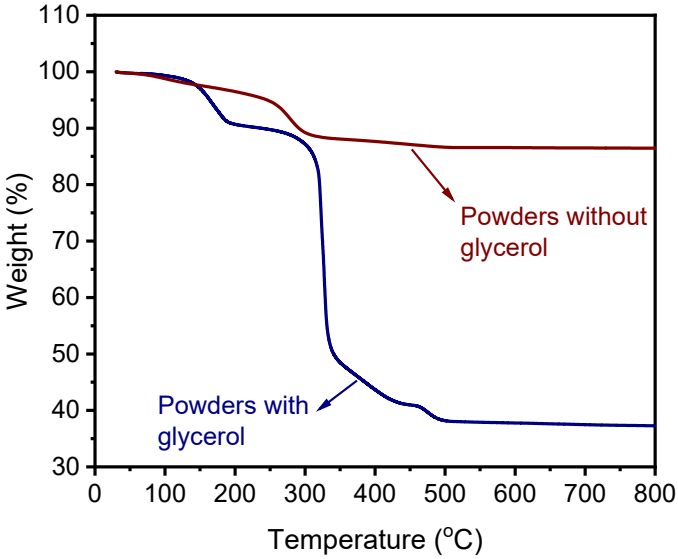

Fig. S11. TG curves of precursor powders synthesized with and without glycerol, respectively.

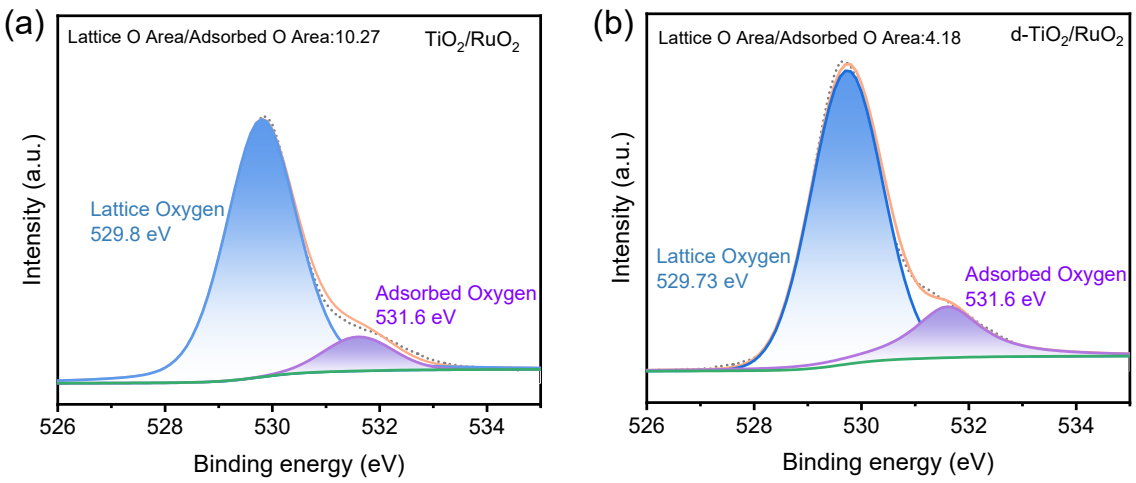

Fig. S12. Fitted O1s XPS signal of (a) TiO_2/RuO_2 and (b) d-TiO_2/RuO_2, respectively.

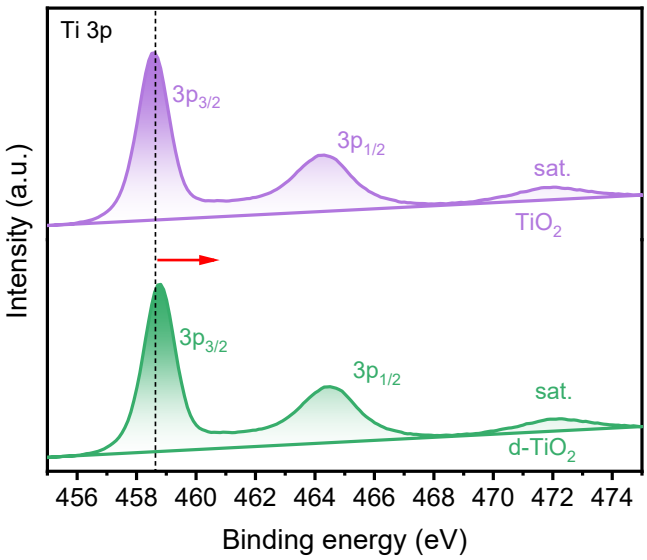

Fig. S13. Ti 3p region for d-TiO_2 and d-TiO_2, respectively.

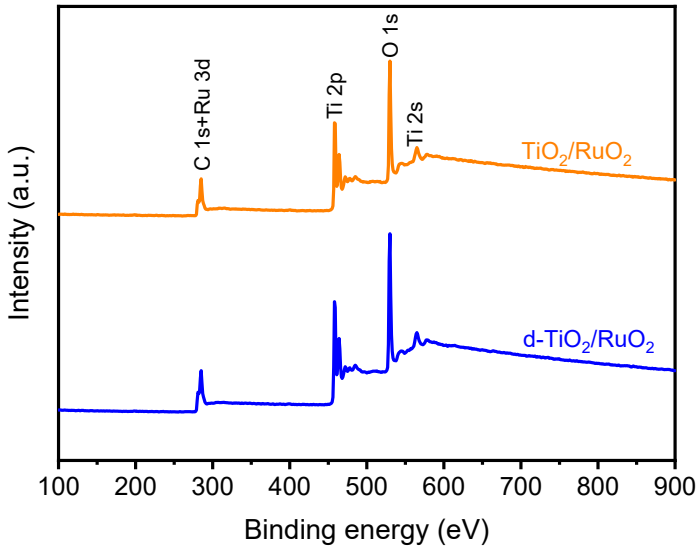

Fig. S14. XPS survey spectra of (a) TiO_2/RuO_2 and (b) d-TiO_2/RuO_2, respectively.

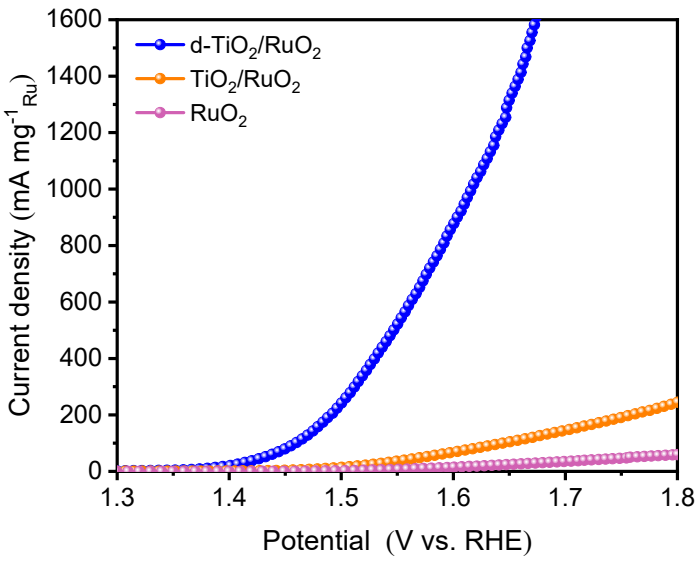

Fig. S15. OER LSV polarization curves normalized by Ru loading of d-TiO_2/RuO_2, TiO_2/RuO_2, and RuO_2, respectively.

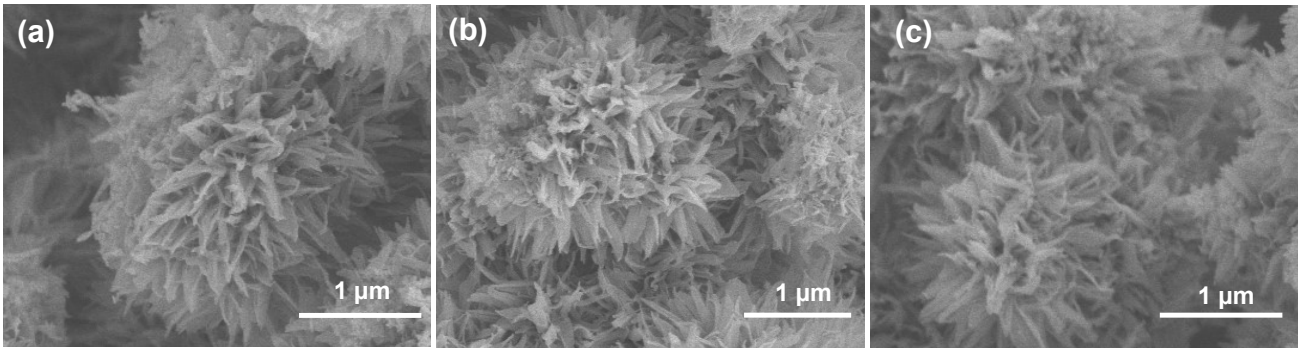

Fig. S16. SEM images of (a) d-TiO_2/RuO_2-1, d-TiO_2/RuO_2-3 and (c) d-TiO_2/RuO_2-7, respectively. All of the samples are nanoflower structures, indicated that the effect of loading on catalyst morphology is negligible.

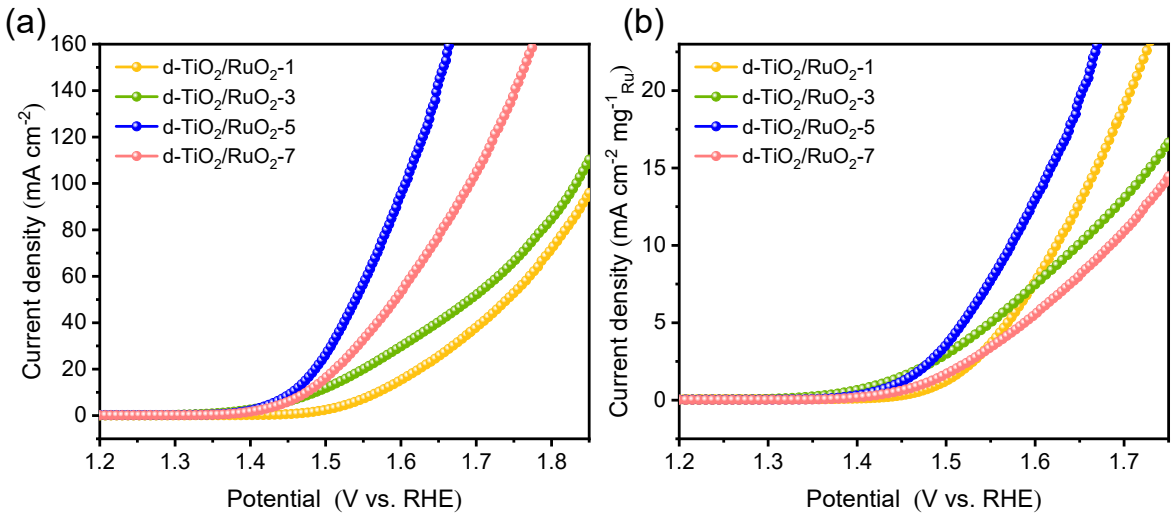

Fig. S17. (a) OER LSV polarization curves of d-TiO_2/RuO_2-1, d-TiO_2/RuO_2-3, d-TiO_2/RuO_2-5 and d-TiO_2/RuO_2-7, respectively. (b) OER LSV polarization curves normalized by Ru loading of d-TiO_2/RuO_2-1, d-TiO_2/RuO_2-3, d-TiO_2/RuO_2-5 and d-TiO_2/RuO_2-7, respectively.

The d-TiO_2/RuO_2-5 exhibits a low overpotential of only 226 mV to achieve the current density of 10 mA cm^{-2}, which is much better than d-TiO_2/RuO_2-1 (339 mV), d-TiO_2/RuO_2-3 (256 mV) and d-TiO_2/RuO_2-7 (245 mV). It is also observed that d-TiO_2/RuO_2-5 also exhibits the best OER activity, even eliminating the effect of loading by mass normalization.

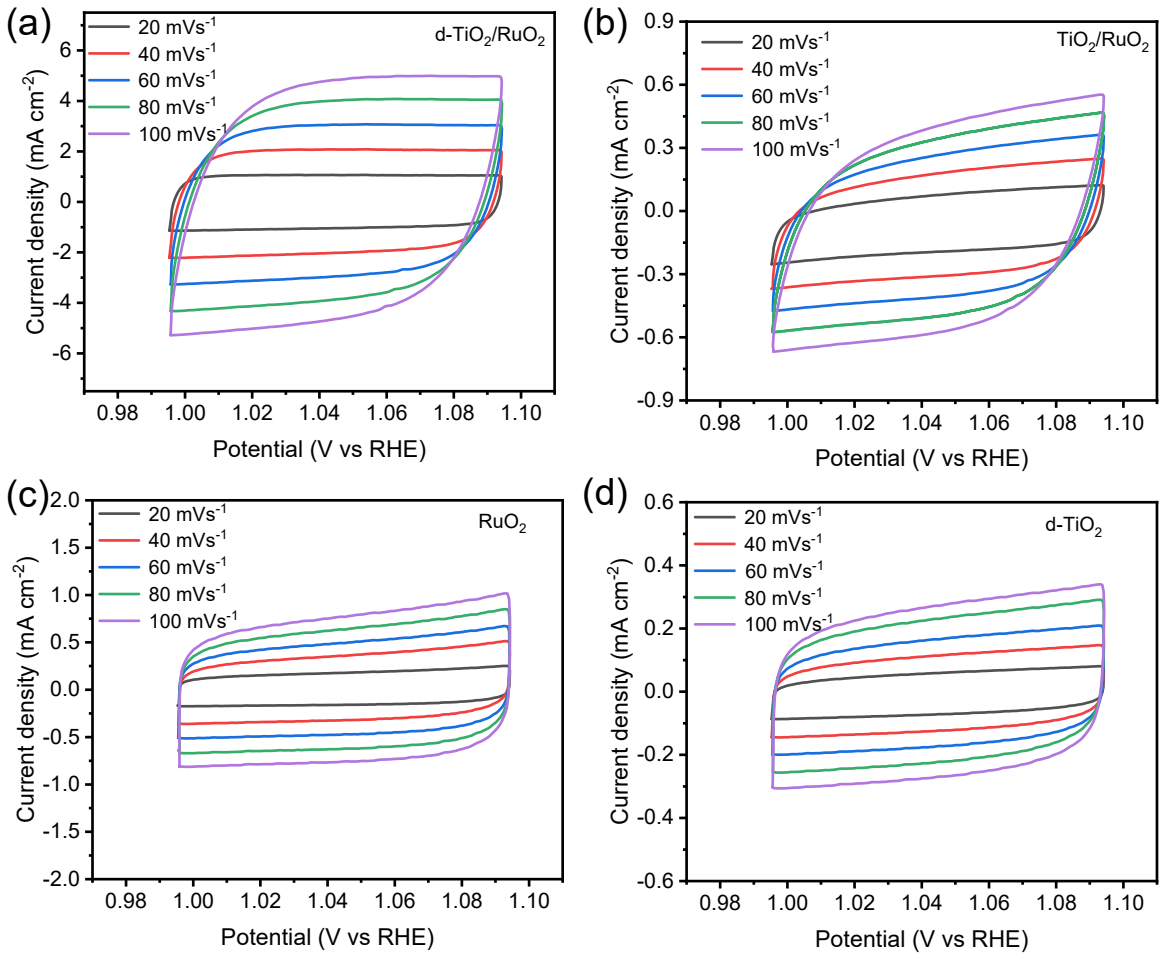

Fig. S18. Cyclic voltammograms of different samples from 20 to 100 mV s^{-1} between 0.995 and 1.095 V, respectively.

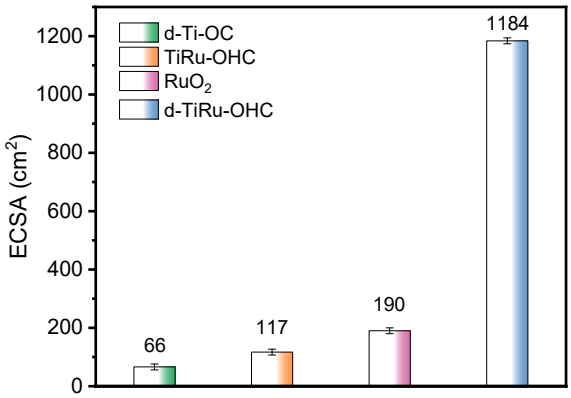

Fig. S19. The ECSA of d-TiO_2/RuO_2, TiO_2/RuO_2, RuO_2 and d-TiO_2, respectively.

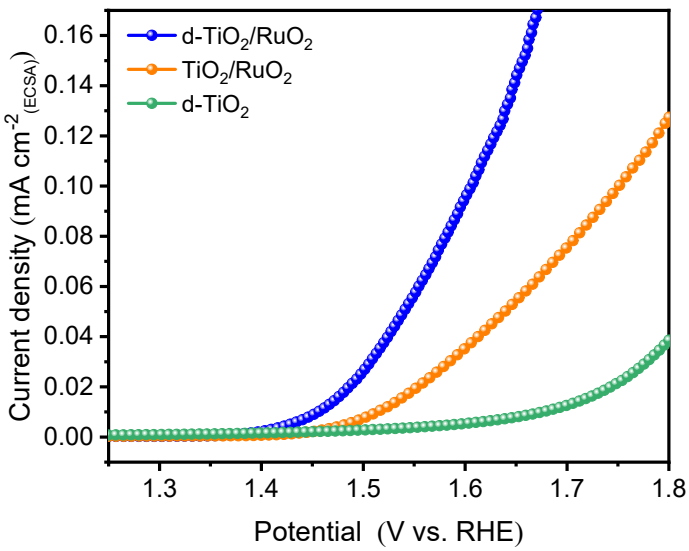

Fig. S20. OER LSV polarization curves normalized by ECSA of d-TiO_2/RuO_2, TiO_2/RuO_2, and d-TiO_2, respectively.

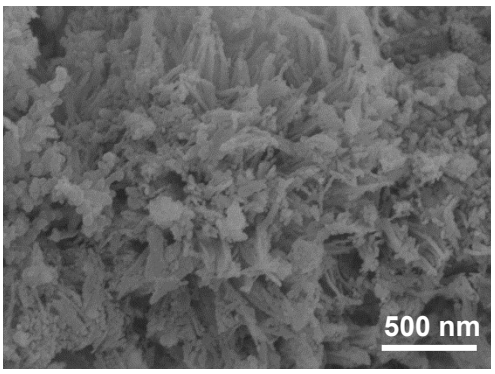

Fig. S21. SEM image of d-TiO_2/RuO_2 after OER at 10 mA cm^{-2} for 10h.

The d-TiO_2/RuO_2 maintained the original morphology. Since carbon black is added as a conductive agent in the preparation of the catalyst for electrochemical testing, a lot of carbon black can be observed on the nanoflowers.

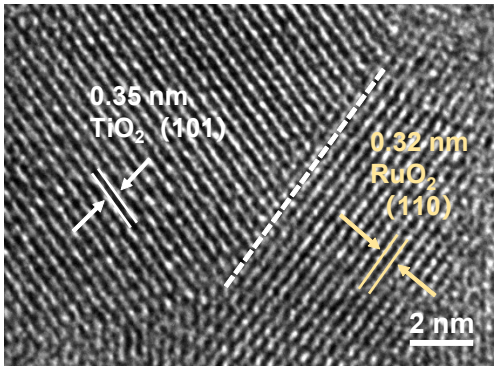

Fig. S22. TEM image of d-TiO_2/RuO_2 after OER at 10 mA cm^{-2} for 10h.

TEM shows the clear interface contact between TiO_2 and RuO_2 after the stability measurement.

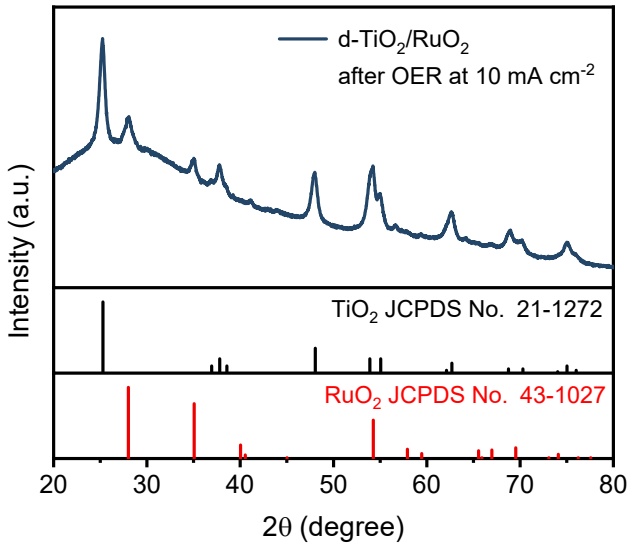

Fig. S23. XRD of d-TiO_2/RuO_2 after OER at 10 mA cm^{-2} for 10h.

The XRD peaks of d-TiO_2/RuO_2 correspond well with both phases of anatase TiO_2 (JCPDS NO.21-1272) and rutile RuO_2 (JCPDS NO.43-1027), which indicated that there is no phase change for d-TiO_2/RuO_2.

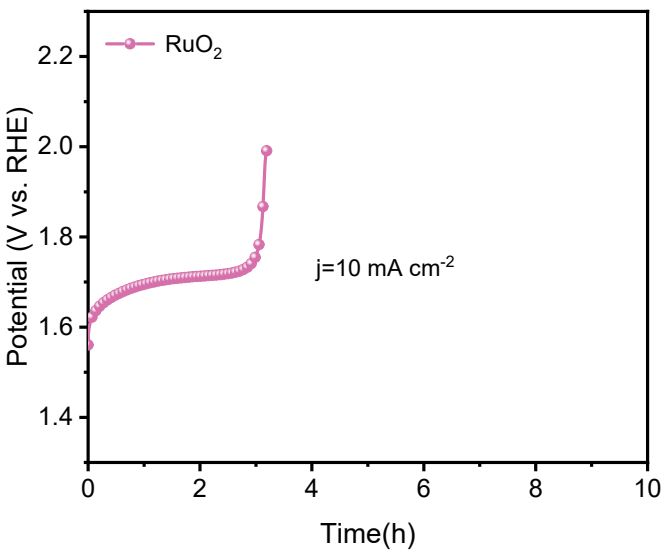

Fig. S24. The chronopotentiometry measurement of RuO_2 at 10 mA cm^{-2}.

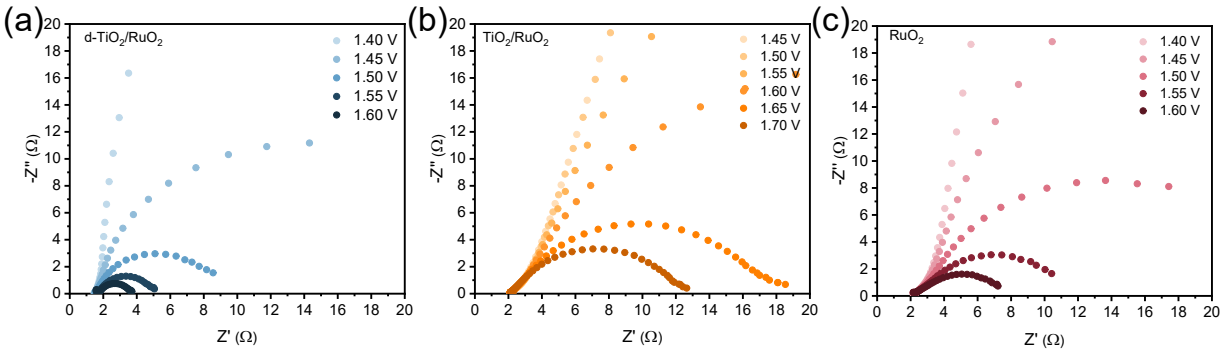

Fig. S25. In operando EIS of d-TiO_2/RuO_2, TiO_2/RuO_2, and RuO_2 collected under different polarization potentials (the applied potential is referenced to RHE). The corresponding Nyquist plots for (a) d-TiO_2/RuO_2, (b) TiO_2/RuO_2, and (c) RuO_2, respectively.

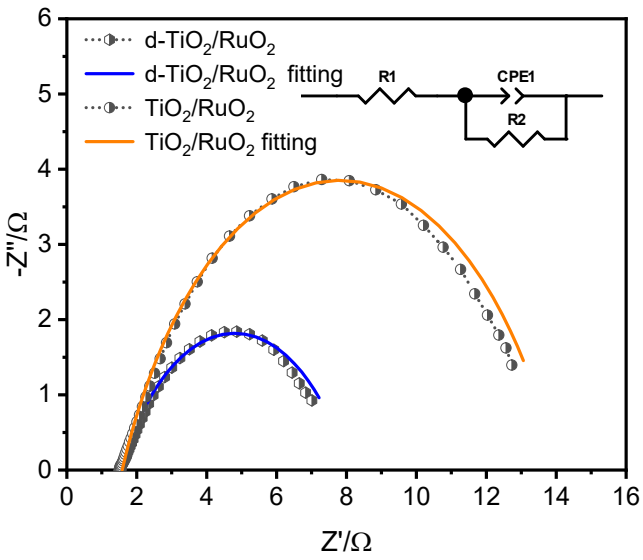

Fig. S26. EIS curves for d-TiO_2/RuO_2 and TiO_2/RuO_2. The inset shows equivalent circuit models for OER.

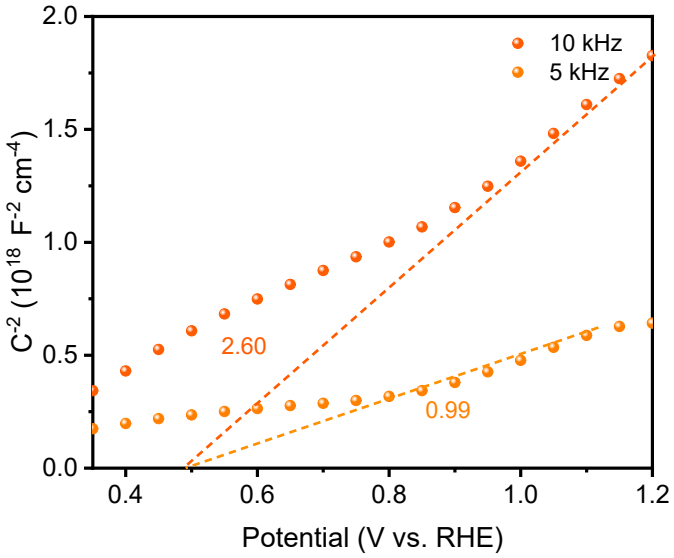

Fig. S27. Mott-Schottky curves of TiO_2/RuO_2.

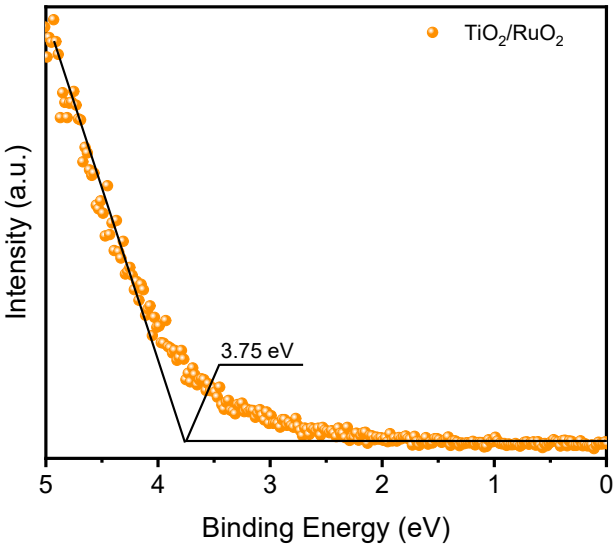

Fig. S28. UPS valence-band spectra of TiO_2/RuO_2.

Table S1. Inductive Coupled Plasma (ICP) results of prepared samples.

Samples	Ti (wt.%)	Ru (wt.%)
d-TiO_2/RuO_2	58.09	2.42
TiO_2/RuO_2	58.18	2.31
d-TiO_2/RuO_2-1	66.78	0.45
d-TiO_2/RuO_2-3	58.09	1.33
d-TiO_2/RuO_2-7	55.70	3.57

Table S2. Comparison of overpotential (10 mA cm^{-2}) and Tafel slopes for OER between d-TiO_2/RuO_2 and various reported catalysts.

Catalyst	**η_{100} (mV)**	**References**
d-TiO_2/RuO_2	226	This work
a-$RuTe_2$	245	Nat. Commun. 2019, 10, 5692
RuO_2 Nanosheet	250	Adv. Energy Mater. 2019, 9, 1803795
RuO_2-$NaPO_3$	250	Curr. Nanosci. 2017, 13
1D-RuO2-CN_x	250	ACS Appl. Mater. Interfaces 2016, 8, 28678-28688
0.27-RuO_2@C	250	Nano Energy 2019, 55, 49-58
RuOOH	255	Adv. Energy Mater. 2019,9, 1803795
PDO-RuO_2	257	ACS Appl. Mater. Interfaces 2019, 11, 42298-42304
SS PtRuO_2 HNSs	260	Sci. Adv. 2022,8, eabl9271
Ru-N-C	267	Nat. Commun. 2019, 10, 4849
RuO_2/$(Co,Mn)_3O_4$/CC	270	Appl. Catal B-Environ. 2021, 297, 120442
IrO_2@RuO_2	270	J. Phys.Chem. C 2016, 120, 2562-2573
RuO_2@C@SiO_2	280	ACS Appl. Mater. Interfaces 2017, 9, 2387-2395
IrO2-RuO2@Ru(3:1)	281	J. Mater. Chem. A. 2017, 5, 17221-17229
Ru@IrO_x	282	Chem 2019, 5, 445
Ru-SA/$Ti_3C_2T_x$	290	Small 2020, 16, e2002888
$Y_{1.85}Zn_{0.15}Ru_2O_{7-x}$	291	Appl. Catal. B: Environ. 2019, 244, 494-501

RuIr@CoNC	300	ACS Catal. 2021, 11, 3402
$RuNiO_x$	386	J. Energy Chem. 2023, 77, 54-61
Mn/TiO_2-RuO_2	386	Appl. Catal B-Environ. 2020, 261 118225

Table S3. Overall water splitting fitting results of EIS for d-TiO_2/RuO_2 and TiO_2/RuO_2.

Catalysts	Rs (ohm)	Rp (ohm)	Error (%)
d-TiO_2/RuO_2	1.15	6.52	0.59
TiO_2/RuO_2	1.58	12.45	0.59